Helium atom scattering from isolated CO molecules on copper(001)

A. P. Graham, F. Hofmann, and J. P. Toennies
M.P.I. für Strömungsforschung, Göttingen, Germany

J. R. Manson
Department of Physics and Astronomy, Clemson University, Clemson, South Carolina 29634

(Received 29 January 1996; accepted 15 April 1996)

Angular distributions have been measured for helium atoms scattering from isolated CO molecules chemisorbed on a Cu(001) surface as a function of incident beam energy between 9.4 and 100 meV and surface coverage from 1.3% ML to 9.3% ML. Up to five oscillations are clearly observed in the angular distributions. The parallel wave vector transfers of the peaks vary only slightly with incident energy and are independent of coverage up to 20% of a $c(2\times2)$ layer. New hard wall scattering calculations show that all of the distinct peaks observed can be explained by interference structures involving both Fraunhofer diffraction and illuminated face scattering from CO molecules with an approximate hard wall radius of 2.4 Å with no evidence of the classical rainbows predicted in several recent theoretical studies. © *1996 American Institute of Physics.* [S0021-9606(96)00628-9]

I. INTRODUCTION

One of the paramount aims of current surface science is to achieve a microscopic understanding of the structure and dynamics of molecules on surfaces. The invention of the scanning tunneling microscope has brought this goal much closer to realization and it is now possible to ''see'' single molecules on surfaces.[1] The quantitative interpretation is, however, fraught with difficulties. Helium atom scattering (HAS), on the other hand, can, at least for simple systems, also detect and probe single adsorbed molecules and has the advantages that (1) the interactions of the probe are rather well understood and (2) the dynamics can also be investigated.[2] In the present experimental study we report on a detailed investigation of the diffraction of helium atoms from isolated single CO molecules on the Cu(001) surface. The aim has been to further improve our understanding of the interaction potential between the He atoms and the chemisorbed CO molecules.

The first calculations of the differential reflection coefficient for the scattering of atoms from isolated adsorbates on a smooth surface as a function of the scattering angle away from specular were reported in 1984 by Gerber, Yinnon, and Kosloff[3] and in the following year by Heuer and Rice.[4] The intensity oscillations with scattering angle predicted by these calculations were then first observed with helium scattering by Lahee *et al.*[5] for the case of CO on Pt(111). The same authors were able to fully explain the three maxima observed at large parallel wave vectors of about 5, 7, and 10 Å^{-1} in terms of reflection symmetry interferences. These measurements have stimulated further studies by several theoretical groups. Yinnon, Kosloff, and Gerber[6] found, on the basis of classical trajectory calculations, that additional peaks due to single and double collision rainbows should also be present. More recently full wave-packet calculations by Carré and Lemoine[7,8] in 1994 confirmed the results of Yinnon *et al.*,[3,6] and even proposed that the structures seen by Lahee *et al.*[5] may well have been due only to rainbow structures. In view of the extreme sensitivity of the angular distributions to the geometry of the adsorbates as well as to the detailed nature of the interaction, we report here on a more extensive series of experiments for CO on Cu(001) to clarify the origin of the oscillations.

To distinguish between the two mechanisms, the new measurements of angular distributions were carried out for a wide range of incident helium atom beam energies. Whereas the positions of the diffraction peaks are expected to remain at fixed parallel wave vectors (ΔK) as the incident beam energy is varied, the rainbow peaks stay at fixed angles and are consequently shifted to higher ΔK values as the incident beam energy is increased.[6] In the current results, since the parallel wave vectors of the peaks do not shift appreciably with the incident beam energy, they are attributed to diffraction interferences and are not due to rainbows. Hard hemisphere scattering calculations show that all of these peaks arise from interferences between Fraunhofer diffraction and illuminated face scattered amplitudes, both of which are reflected from the surrounding flat metal surface, and thus interfere with each other a second time. Although referred to in the recent literature simply as Fraunhofer oscillations we prefer to designate them as reflection symmetry interferences (RSI)[5,9] because of the complex nature of the interferences. The best fit effective hard sphere radius is found to increase from 2.15 to 2.60 Å with increasing collision energy from 9.4 to 100 meV. This surprising result appears to arise from the difference in softness between the He–CO and He–Cu(001) potentials. A new feature is found at small ΔK which is attributed to an effect of the long range attractive potential.

The present article begins with a brief description of the experimental apparatus and procedures. In Sec. III we present the experimental results, followed by the new theoretical model used to analyze the data in Sec. IV. The results are then analyzed and discussed in Sec. V, with a summary and outlook presented in Sec. VI.

II. EXPERIMENTAL DETAILS

The high resolution ($\Delta E/E \approx 2\%$) helium scattering apparatus used in these experiments has been described elsewhere.[10] Incident beam energies between 9.4 and 100 meV were achieved by varying the source temperature between 62 and 450 K. A fixed angle of $\theta_{SD}=95.8°$ between the incident beam direction and the final scattering direction seen by the detector was used for all of the experiments described here. The angular distributions were obtained by rotating the polar angle of the sample manipulator, which is orthogonal to the incident beam-detector plane. The parallel wave vector is given by $\Delta K = k_i \sin\theta_i - k_i \sin\theta_f$. The measurement of a complete angular distribution required typically 20 min.

The experiments were performed on a Cu(001) single crystal aligned to an accuracy of $<0.25°$, mechanically polished, and inserted into the vacuum system on a six-axis sample manipulator. *In vacuo* cleaning of the sample involved argon ion bombardment at 750 V and 1 μA cm^{-2} and annealing cycles to 750 K to remove bulk and surface contamination. A contamination level of less than 0.5% was determined with Auger spectroscopy and confirmed by elastic and inelastic helium scattering.

Carbon monoxide exposure was carried out at 120 K by backfilling the sample chamber to a pressure of 1×10^{-8} mbar with 99.997% pure CO gas,[11] while the coverage was monitored using specular helium attenuation as described by Ellis, Witte, and Toennies.[12] Throughout the text, all coverages reported refer to the Cu(001) atom density [$c(2\times2)$ corresponds to $\Theta=50\%$ ML]. The error in absolute coverage is estimated to be 0.5% ML. The surface temperature was measured with a standard Ni–CrNi thermocouple attached to the side of the singe crystal. To reduce the probability of inelastic scattering processes the sample was maintained at a temperature $T_s=50$ K during the measurement of the angular distributions. The sample chamber vacuum was $<2\times10^{-11}$ mbar during the experiments and there was no evidence for buildup of contamination despite the low surface temperatures.

III. RESULTS

In the present investigation only angular distributions of the total signal were measured although, in fact, complete information concerning the single adsorbate structure is best extracted from measurements of only the elastic channel. In addition to the phonons of the surface, the helium atoms also couple strongly to the frustrated translation mode (T mode) of the isolated CO molecules which has an energy of $\hbar\omega \approx 4$ meV.[9] A previous study revealed that at $T_s=111$ K the same oscillations occur both in the elastic and single-phonon T-mode annihilation and creation channels[9] but with different phases. Since the signals in the inelastic channels are a factor of 30 less than the elastic channel for $\Delta K \leqslant 2.5$ Å^{-1}, the smearing effect is small. Thus the much greater measuring time required for a full time-of-flight (TOF) analysis did not seem warranted. The small smearing effect of the predominant annihilation channel was further suppressed by lowering the surface temperature to $T_s=50$ K. Inelastic TOF measurements performed at key angles in the angular distribution also confirmed that the largest variation in the total signal arises from oscillations of the elastic signal with angle.

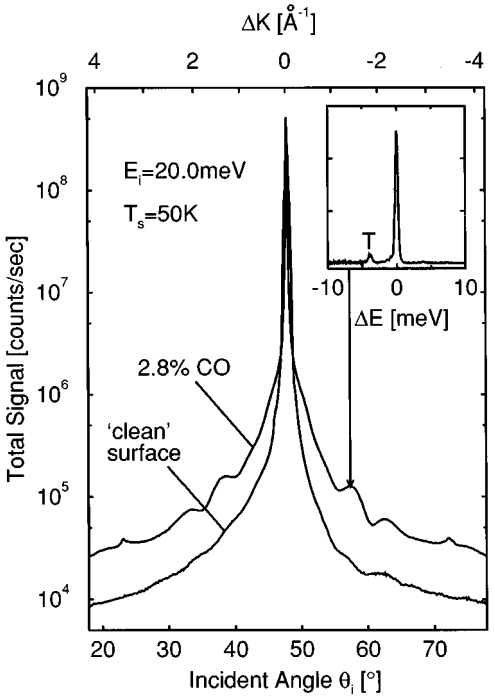

FIG. 1. The total signal angular distributions (logarithmic scale) for the clean Cu(001) surface is compared with a 2.8% ML CO coverage measured along the [100] direction. The incident beam energy was 20 meV ($k_i=6.19$ Å^{-1}) and the surface temperature was 50 K. A time-of-flight spectrum for an incident angle of 58° converted to an energy transfer scale shown in the inset indicates that the scattering is dominated by the elastic channel.

In Fig. 1 the angular distribution of the total signal plotted on a logarithmic scale for 2.8% ML CO coverage is compared with the clean surface under the same conditions. Note the large range of signals encountered in going from the specular peak ($\sim3\times10^8$ counts/s) to the largest angles ($\sim10^4$ counts/s), corresponding to more than four orders of magnitude change. It should also be noticed that the structures are sharpest on the large incident angle side of the specular peak. At these angles the small remaining contribution from inelastic T-mode creation events, seen at negative ΔE in the energy transfer spectrum shown in the inset of Fig. 1, is suppressed compared to the elastic scattering events. From Fig. 1 it is seen that the total signal increases upon CO adsorption by a factor of 3–5 at angles greater than a few degrees away from the specular position. The clean surface angular distribution also displays several very weak oscillations at $\theta_i \approx 57°$ and $\theta_i \approx 62°$. These peaks lie in the same positions observed for CO on the surface, and are incompatible with the positions anticipated for scattering from steps.[13] Therefore, we assign these oscillations to a small quantity of CO adsorbed from the residual gas in the ultrahigh vacuum chamber during the period of about 30 min that the sample was cooled and maintained at 50 K. In the following discus-

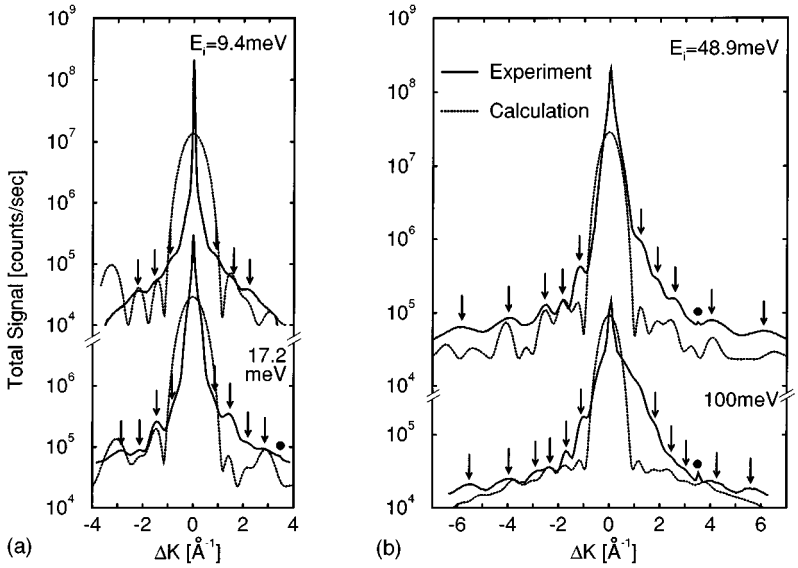

FIG. 2. A series of angular distributions (logarithmic scale) for different incident beam energies for scattering from 2.8% ML CO on a Cu(001) surface in the [100] direction. The incident beam energies have been calibrated using time-of-flight measurements. (a) shows distributions for incident energies from 9.4 to 20.0 meV while (b) shows distributions for incident energies from 30 to 100 meV. The positions of maxima are indicated by pointers (↓) and diffraction peaks are indicated by filled circles (●). The dashed lines accompanying each distribution indicate a theoretical fit to the measurement using the hybrid hard-hemisphere scattering calculation described in Sec. IV for the best value of the object radius.

sion the angular distributions are presented as measured. For identification of the peaks they were converted into a parallel wave vector (ΔK) abscissa using values of k_i measured in TOF experiments before each distribution was recorded. $\Delta K>0$ (forward scattering) corresponds to $\theta_i<47.9°$ and $\Delta K<0$ (backward scattering) to $\theta_i>47.9°$.

Figure 2 shows a series of four logarithmic total signal angular distributions for incident beam energies from $E_i=9.4$ meV ($k_i=4.24$ Å^{-1}) to $E_i=100$ meV ($k_i=13.8$ Å^{-1}) plotted against ΔK. All of the angular distributions are dominated by a very intense specular peak with a total signal of around 3×10^8 counts/s at 9.4 meV which decreases to 8×10^6 counts/s at 100 meV.

The parallel wave vector distributions have at least two, and up to six, distinct peaks on each side of the specular. All of the distributions have a peak at $\Delta K\approx1.4$ Å^{-1} and another at $\Delta K\approx2.0$ Å^{-1}. These peaks vary slightly in parallel wave vector with incident beam energy, decreasing from 1.5 to 1.1 Å^{-1} and 2.1 to 1.7 Å^{-1}, respectively, as the beam energy is raised from 9.4 to 100 meV. The incident angles corresponding to these peaks are seen to decrease significantly, however, from $\pm15°$ to $\pm6°$ and from $\pm22°$ to $\pm8°$, respectively, relative to the specular angle, in the same range of incident energies. Some of the peaks at larger wave vectors, particularly at higher incident energies, are not evident in all of the spectra. Examination of Fig. 2 reveals an increase in the sharpness of the structures in going to higher incident energies. At an incident energy of 100 meV at least six peaks are clearly resolved for $|\Delta K|\gtrsim0.8$ Å^{-1}.

In some of the angular distributions sharp peaks indicated by filled circles (●) are seen at $\Delta K=3.5$ Å^{-1}. These peaks lie at the Cu(001) diffraction positions for the [100] surface direction used in the measurements. Since in Fig. 1 the diffraction intensities from the CO covered surface at $\Delta K\approx3.5$ Å^{-1} are much stronger than those from the clean surface, we attribute these peaks to scattering from the lattice gas of CO molecules occupying identical adsorption sites which have been identified as on-top sites.[14] Diffraction from a lattice gas of CO molecules can also explain the small variation of the specular and lattice diffraction peak intensities with changing incident beam energy. Since the other scattering interference structures were found to be independent of the crystal azimuthal orientation they are not the result of lattice gas diffraction.

The effect upon the angular distribution structures of increasing adsorbate coverage in going from 1.3% to 9.3% ML is shown in Fig. 3 for an incident beam energy of 40 meV. The distributions in Fig. 3 show that the total signal of the angular peaks increases with coverage, as anticipated for an increase in the number of scattering centers. Most important, the positions of the peaks are independent of the adsorbate density, at least up to 10% ML. This indicates that the CO molecules chemisorbed on the surface are randomly distributed on lattice sites. If they were to assume a long range ordered structure, then similar structures due to diffraction which shift to larger ΔK values with increasing coverage would be seen. This phenomenon has been observed for several different adsorbates such as alkali atoms on low index copper and nickel surfaces in our laboratory.[15–17]

IV. SCATTERING THEORY

The energy range and scattering geometry used in these experiments imposes severe restrictions upon the calculations which can be used to model the reflection symmetry oscillations. In particular, the relatively high incident beam

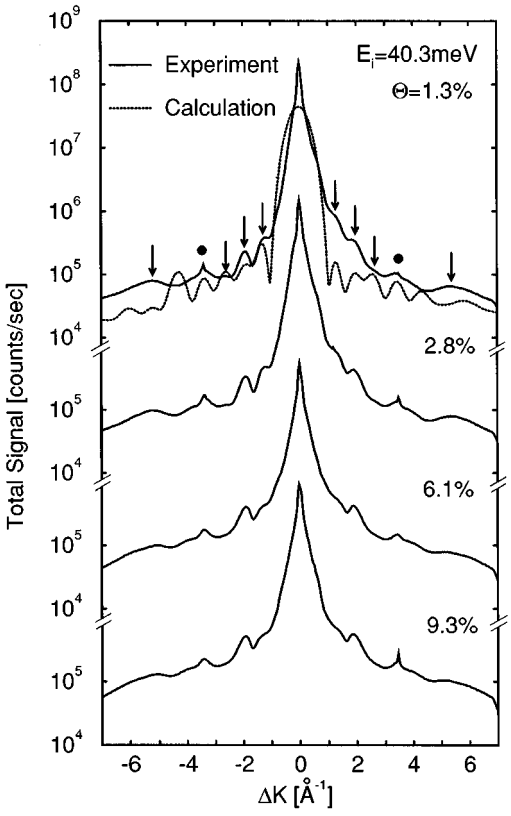

FIG. 3. A series of angular distributions for helium atoms scattered from CO adsorbed on Cu(001) with different CO coverages along the [100] direction. An incident beam energy of 40 meV was used and a surface temperature of $T_R = 50$ K. Note that the oscillations become stronger with coverage, but that the major peak positions, indicated by pointers (↓), do not change. The filled circles (●) indicate reciprocal lattice points of the Cu(001) lattice.

energies and non-normal incident angles used prevent a wave-packet calculation from being performed in a simple manner.[8] The non-normal incident angle also weakens the sudden approximation approach, which works best for incident and final scattering angles close to the surface normal.[18] Therefore, we have used a hard-wall scattering solution to model the helium scattering results.

As discussed previously,[5,9] the quantum mechanical scattering of helium atoms from an isolated adsorbate on a smooth surface can be treated using the reflection construction. The scattering amplitude in the semiclassical limit contains two contributions: (a) a direct scattering contribution involving only the adsorbate, and (b) a contribution involving second scattering from the mirror surface. The total scattering amplitude is thus given by

$$F(\theta_i,\theta_f) = f_a(|\theta_i - \theta_f|) - f_b(\pi - \theta_{\mathrm{SD}}), \tag{1}$$

where θ_i, θ_f and θ_{SD} are the incident, final, and total $(\theta_i + \theta_f)$ scattering angles respectively. Next we note that there are two contributions to f_a and f_b in Eq. (1). One contribution, which is designated f_{face} accounts for the predominantly wide angle scattering from the illuminated face of the boss. The other term, designated $f_{\mathrm{Fraunhofer}}$, accounts for the predominantly forward scattered Fraunhofer diffraction. Next we note that the intensity of the scattered helium atoms is given by

$$I(\theta_i,\theta_f) = |F^2|. \tag{2}$$

Thus since altogether four terms contribute to F there will be six additional interference terms.

In the past formulations[5,9] and in the present work the actual interaction potential between the helium atom and the CO molecule is approximated by a hard wall. In our two previous studies of isolated CO molecules on metal surfaces, two different scattering approximations were used. Lahee *et al.*[5] used the Kirchoff approximation to describe the illuminated face amplitude (F_{face}) for a hard hemispherical potential and an analytical formula for the Fraunhofer diffraction amplitude ($F_{\mathrm{Fraunhofer}}$) to qualitatively reproduce the interference effects observed experimentally for CO on Pt(111). Later, Bertino *et al.*[9] used the Eikonal approximation to calculate the Fraunhofer and illuminated face components of the scattered intensity for both f_a and f_b to model both elastic and inelastic scattering from isolated CO molecules adsorbed on Cu(001).

The Kirchoff approximation used by Lahee *et al.*[5] applies when $R_0 \gg \lambda_i$, where λ_i is the incident beam wavelength and R_0 is the radius of the object on the surface. For the lowest incident energies of ~10 meV (1.4 Å) and the observed object radii (~2.5 Å) used here, $\lambda_i/R_0 \sim 0.6$ and the calculation cannot be expected to accurately reproduce the illuminated face component of the interaction. Moreover, in the previous calculation by Bertino *et al.*,[9] the Fraunhofer component of the scattering amplitude was calculated using the Eikonal approximation[19] in a formulation which is, strictly speaking, only exact for normal incidence.

As a consequence of these shortcomings we have adopted a new hybrid approach. The Eikonal approximation is used to calculate the illuminated face component of the scattering amplitude using a hard hemisphere with a corrugation function denoted by $\xi(R)$. This term is modified by Eq. (1) to account for reflection by the surface

$$F_{\mathrm{face}}(\theta_i,\theta_f) = ik_i \cos\theta_f \int_0^{R_0} J_0(\Delta K R)[e^{-i(k_{iz}-k_{fz})\xi(R)} - e^{-i(k_{iz}+k_{fz})\xi(R)}]RdR, \tag{3}$$

where J_0 is an ordinary Bessel function, k_{iz} and k_{fz} are the normal components of the incident and final helium atom momenta, respectively, and ΔK is the parallel wave vector. In Eq. (3) integration over the entire boss in two dimensions has been reduced to an integration in radius only because the integral over polar angle can be trivially carried out.

The predominantly forward scattered Fraunhofer component to the scattered amplitude is calculated here using the analytical formula used by Lahee *et al.*,[5] which also applies for finite angles of incidence

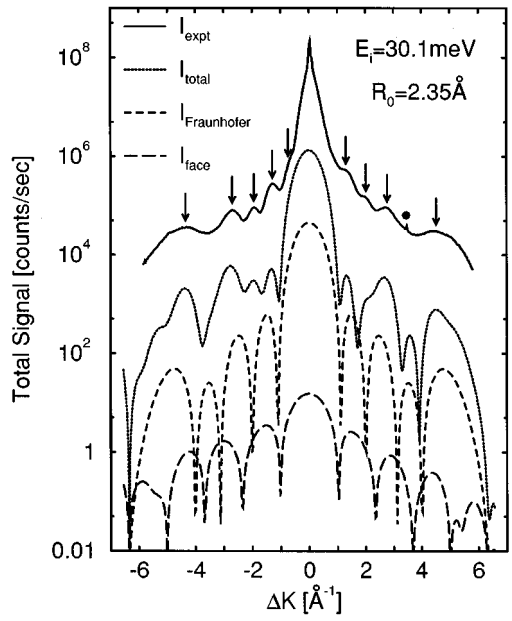

FIG. 4. The result of hybrid eikonal calculations for a hard hemispherical boss of radius $R_0=2.35$ Å for an incident beam energy of 30.1 meV. The top (solid) curve shows the experimental angular distribution. The remaining curves show the various component intensities of the total calculated intensity (dotted curve), Fraunhofer interference (dashed curve) intensity, and illuminated face intensity (long-dashed curve). Each curve has been reduced in intensity by a factor of 10 for clarity.

$$f_{\text{Fraunhofer}}(\theta_i,\theta_f) = \frac{iR_0}{2}\left[\frac{(1+\cos(|\theta_i-\theta_f|))J_1(k_i a\ \sin(|\theta_i-\theta_f|))}{\sin(|\theta_i-\theta_f|)}\right], \quad (4)$$

where J_1 is an ordinary Bessel function and R_0 is the radius of the hemispherical boss. The second term in Eq. (1) (f_b) is obtained by replacing ($|\theta_i-\theta_f|$) in Eq. (4) by ($\pi-\theta_{\text{SD}}$). In this formalism only one free parameter, namely the object radius R_0 remains. All other terms are fixed by the kinematical conditions.

V. DISCUSSION

The hybrid calculation has been used to evaluate the experimental results presented in Sec. III. A typical best fit calculation for 30 meV incident energy can be seen in Fig. 4 for an object radius of 2.35 Å. The separate contributions from the Fraunhofer intensity $I_{\text{Fraunhofer}}$ reflected from the surface and the illuminated face intensity I_{face} also reflected from the surface are both shown. The calculation of the total intensity with interference between these two contributions shows that none of the calculated peaks arises solely from Fraunhofer diffraction. Note that in the present calculations the illuminated face intensity shows a significant interference structure whereas in previous work[5] this did not appear in the calculations. Thus, this effect is not reproduced accurately by the analytical expression for the illuminated face component derived in the Kirchoff approximation.[5] Therefore all four components are important for a complete calculation of the full interference pattern. Best fit calculations of the total intensity from the interference oscillations are shown for each incident beam energy in Fig. 2. With the exception of the weak shoulder at $\Delta K\approx 0.8$ Å^{-1} the fit of both intensity and position to the experimental results is very satisfactory. The best fit radius of 2.35 Å at 30.1 meV is very close to that expected from the height of the CO molecule derived from the sum of He–surface and He–CO pair potentials [$R_0\approx 2.5$ Å at 30 meV (Ref. 20)], and is in reasonable agreement with the values of $R_0=2.5$ Å determined by Lahee *et al.* for CO/Pt(111) at $E_i=42$ meV,[5] and $R_0\approx 2.3$ Å for CO/Cu(001) at $E_i=42$ meV (Ref. 9) obtained previously with the more approximate scattering theories.

On the basis of the good fit achieved with the model we conclude that there is indeed, at present, no convincing experimental evidence for a single scattering rainbow structure for this system. In this connection it is worth noting that the hard-wall hemispherical shape used here does not have an inflexion point in the corrugation and therefore cannot produce a single scattering rainbow at large angles.[19] Thus, the shape assumed here, which rules out single scattering rainbows, is justified by the experiments. However, in contrast, the wave-packet calculations of Carré and Lemoine[7] for a soft potential with a long range attractive potential predict a single scattering rainbow peak for incident beam energies above 8 meV.

Several experimental distributions show distinct shoulders on both sides of the specular at $\Delta K\sim 0.8$ Å^{-1}, particularly at low incident energy which cannot be predicted by the present calculation. These shoulders could indicate the presence of an additional peak such as those calculated by Yinnon, Kosloff, and Gerber[6] and Carré and Lemoine.[7] While we cannot rule out the possibility of a double scattering event perturbed by the attractive part of the He–CO potential,[6] our calculations indicate that it is unlikely that this feature comes from reflection symmetry interferences, as the hard core radius required would be too large. More likely the shoulders are due to an effect of the long range attractive van der Waals interaction on the trajectory of the helium atoms. A similar effect has been seen in angular distributions from free N_2 molecules in molecular beam scattering experiments[21] and is found to be especially prominent at low collision energies as observed here (see Fig. 2). According to this mechanism, the helium atoms which would otherwise miss the molecule, are refracted through small angles by the long range attractive part of the potential, and thus this shoulder can be looked upon as a vestige of the classical rainbow. Naturally this refraction applies to helium atoms hitting the molecule as well. Thus it may be, in part, responsible for the observed energy dependence of R_0 discussed next.

The best fit values of the radius R_0 for each incident energy are tabulated in Table I. Surprisingly, the effective radius R_0 increases with beam energy E_i monotonically instead of decreasing as expected for scattering from an isolated molecule because of the softness of the potential. In another type of He-atom interference experiment Ellis *et al.*[20] found an increase in CO island height with incident

TABLE I. Best fit hemispherical boss radii against incident beam energy using the hybrid calculation.

E_i(meV)	k_i(Å^{-1})	R_0(Å)
9.4	4.24	2.15
11.5	4.69	2.17
14.4	5.25	2.18
17.2	5.74	2.21
20.0	6.18	2.25
30.1	7.59	2.35
40.3	8.78	2.39
48.9	9.67	2.45
66.6	11.29	2.55
100	13.83	2.60

energy, from 2.23 to 2.42 Å over the same incident energy range. This effect could be explained by a difference in the repulsive potential of the clean Cu(001) surface and for scattering from the CO molecules. It is interesting to see that the same trend is observed here. Whereas in the experiment of Ellis *et al.*[20] only the height difference was measured, the present experiment is sensitive to both the height and radius of the boss. For lack of a better theory we are, at present, not able to investigate the relative effect of these two dimensions. In addition, it is not possible to account for the softness of the real potentials and the effect of the long range potential. Thus we can only speculate that the increase in base radius could be the result of an interaction between the copper surface and CO molecule producing an additional ''tail'' to the distribution dictated by the hemisphere hard-wall model. Such a distribution would be interpreted by the Fraunhofer scattering term as an apparent increase in the CO molecule radius with an increase in incident energy. Hence we propose that at small ΔK the experimental angular distributions are highly sensitive to the effective CO molecule height and base radius. Presumably the exact shape of the CO potential could be extracted from the energy dependence measured here with a realistic theory such as that used by Carré and Lemoine.[7,8]

VI. CONCLUSION

In this paper we have presented new results for the energy dependence of interference structures for helium atoms scattered from isolated CO molecules on a Cu(001) surface. A hybrid eikonal hard wall calculation is able to interpret the salient features of the distributions in terms of reflection symmetry interferences.[5] At present it is not clear whether the absence of evidence for rainbow structures is due to the lack of an inflexion point in the potential (as in the hard hemispherical boss used here) or has another origin. A new feature is observed at $\Delta K = 0.8$ Å^{-1} for low incident energies, which is attributed to the attractive van der Waals part of the helium-molecule potential.

The hybrid eikonal calculation predicts an object radius of 2.35 Å at 30 meV, which is in good agreement with the hard core radius derived from a potential summation.[20] In addition, the increase of the radius with incident energy follows the trend predicted from independent measurement of the height of CO islands as a function of incident energy.[20]

ACKNOWLEDGMENT

J.R.M. would like to acknowledge support from the National Science Foundation under Grant No. DMR9419427.

[1] D. M. Eigler, P. S. Weiss, E. K. Schweizer, and N. D. Lang, Phys. Rev. Lett. **66**, 1189 (1991).
[2] F. Hofmann and J. P. Toennies, Chem. Rev. (in press).
[3] R. B. Gerber, A. T. Yinnon, and R. Kosloff, Chem. Phys. Lett. **105**, 523 (1984).
[4] M. Heuer and T. M. Rice, Z. Phys. B **59**, 299 (1985).
[5] A. M. Lahee, J. R. Manson, J. P. Toennies, and Ch. Wöll, Phys. Rev. Lett. **57**, 471 (1986); J. Chem. Phys. **86**, 7194 (1987).
[6] A. T. Yinnon, R. Kosloff, and R. B. Gerber, J. Chem. Phys. **88**, 7209 (1988).
[7] M.-N. Carré and D. Lemoine, J. Chem. Phys. **101**, 5305 (1994).
[8] D. Lemoine, J. Chem. Phys. **101**, 4343 (1994).
[9] M. Bertino, J. Ellis, F. Hofmann, J. P. Toennies, and J. R. Manson, Phys. Rev. Lett. **73**, 605 (1994).
[10] F. Hofmann, J. R. Manson, and J. P. Toennies, J. Chem. Phys. **101**, 10155 (1994); J. P. Toennies, *Springer Series in Surface Sciences*, edited by F. de Wette (Springer, Heidelberg, 1988), Vol. 14, p. 248.
[11] Carbon Monoxide gas bottle supplied by Messer Griesheim, Laboratory gases number 795.07131.
[12] J. Ellis, G. Witte, and J. P. Toennies, J. Chem. Phys. **102**, 5059 (1995).
[13] R. Berndt, B. J. Hinch, J. P. Toennies, and Ch. Wöll, J. Chem. Phys. **92**, 1435 (1990).
[14] S. Andersson and J. B. Pendry, Phys. Rev. Lett. **43**, 363 (1979).
[15] A. P. Graham, F. Hofmann, and J. P. Toennies (unpublished).
[16] J. Braun, J. P. Toennies, and G. Witte (unpublished).
[17] A. P. Graham, F. Hofmann, and J. P. Toennies (unpublished).
[18] J. I. Gersten, R. B. Gerber, D. K. Dacol, and H. Rabitz, J. Chem. Phys. **78**, 4277 (1983).
[19] U. Garibaldi, A. C. Levi, R. Spadacini, and G. E. Tommei, Surf. Sci. **48**, 649 (1975).
[20] J. Ellis, K. Hermann, F. Hofmann, and J. P. Toennies, Phys. Rev. Lett. **75**, 886 (1995).
[21] M. Faubel, J. Chem. Phys. **81**, 5559 (1984).